THE JOURNAL OF PHYSICAL CHEMISTRY B

Article

pubs.acs.org/JPCB

Proton Transfer Dependence on Hydrogen-Bonding of Solvent to the Water Wire: A Theoretical Study

Binh Khanh Mai, Kisoo Park, My Phu Thi Duong, and Yongho Kim*

Department of Applied Chemistry, Kyung Hee University, 1 Seochun-Dong, Giheung-Gu, Yongin-Si, Gyeonggi-Do, 446-701, Korea

Supporting Information

ABSTRACT: The mechanism and dynamics of double proton transfer dependence on hydrogen-bonding of solvent molecules to the bridging water in a water wire were studied by a direct ab initio dynamics approach with variational transition-state theory including multidimensional tunneling. Long-range proton transfers in solution and within enzymes may have very different mechanisms depending on the pK_a values of participating groups and their electrostatic interactions with their environment. For end groups that have acidic or basic pK_a values, proton transfers by the classical Grotthuss and "proton-hole" transfer mechanisms, respectively, are energetically favorable. This study shows that these processes are facilitated by hydrogen-bond accepting and donating solvent molecule interactions with the water wire in the transition state (TS), respectively. Tunneling also depends very much on the hydrogen bonding to the water wire. All molecules hydrogen bonded to the water wire, even if they raised and narrowed energy barriers, reduced the tunneling coefficients of double proton transfer, which was attributed to the increased effective mass of transferring protons near the TS. The theoretical HH/DD KIE, including tunneling, was in good agreement with experimental KIE values. These results suggest that the classical Grotthuss and proton-hole transfer mechanisms require quite different solvent (or protein) environments near the TS for the most efficient processes.

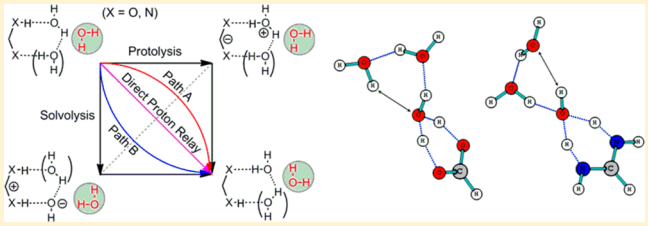

1. INTRODUCTION

Proton transfer is one of the most important reactions in chemical and biological phenomena.[1−4] These reactions can take place over long distances via a hydrogen-bonded network in protic solvents and in proteins.[5−11] Proton relay systems in proteins have become topics of intense theoretical study.[12−16] Water can mediate the long-range transfer of a proton through proton channels, where sequential hopping of protons occurs through hydrogen-bonded (H-bonded) wires. Proton transfer mechanisms and dynamics are also of great importance for acid−base chemistry.[8,17−24] The dynamics of long-range proton transfer is much more complicated than that of a single proton transfer, and its mechanism is not yet fully understood. Water is considered to play a key role in acid−base neutralization reactions in aqueous solution, where a proton is exchanged between an acid and a base, resulting in the conjugate base and conjugate acid, respectively. Proton transfer reactions between acids and bases in aqueous solution may involve different reaction pathways and dynamics, depending on the H-bonding structure of the solvent molecules between the reactants. In typical acid−base reactions, it has been estimated that on average 2−3 water molecules are involved in the proton transfer between an acid and base.[25]

Recently Mohammed et al.[26,27] measured the proton transfer through water bridges between an excited photoacid and several carboxylate bases in aqueous solution and suggested that the proton transfer occurs by a sequential Grotthuss-type hopping mechanism through the H-bond network of the solvent. A classical Grotthuss mechanism[28] is commonly assumed, where sequential "proton hops" between the initial donor and ultimate acceptor are mediated by water molecules and other ionizable groups. Eigen suggested that proton transfer in aqueous solution can occur in three ways:[29] proton transfer from an acid to water, followed by proton abstraction by a base (protolysis), direct proton relay from an acid to a base, and proton transfer from water to the base, with subsequent proton transfer from the acid to the anionic solvent (solvolysis).

Riccardi et al.[30] have performed hybrid quantum mechanical/molecular mechanical (QM/MM) simulations to investigate solvent-mediated proton transfer between simple solutes in water and discussed the long-range proton transfer mechanisms for enzymes. They suggested that long-range proton transfers in solutions and enzymes can exhibit very different molecular details depending on the pK_a values of participating groups and electrostatic interactions with the environment. When the end groups have acidic or basic pK_a values, the classical Grotthuss mechanism and solvolysis (deprotonation of the water molecule first to generate a solvated hydroxide) are energetically more favorable, respectively. Therefore, they argued that the classical Grotthuss mechanism is likely an oversimplifica-

Received: October 30, 2012
Revised: December 12, 2012
Published: December 12, 2012

tion, and the possibility of "proton-hole" transfers[31] should be an important consideration as well.

When proton exchanges in aqueous solution involve a change in charge density, solvent structures near mediating water molecules must play an important role in determining the dynamics of the proton transfer process. Therefore, a reliable theoretical model of long-range proton transfer in solution should consider the pK_a values of the donor and acceptor as well as the solvent structures of mediating groups. Take a simple system in which a proton is transferred between an acid and base through a number of mediating water molecules as illustrated in scheme 1 for three possible processes: protolysis, solvolysis (proton-hole transfer), and the Grotthuss mechanisms.

Scheme 1

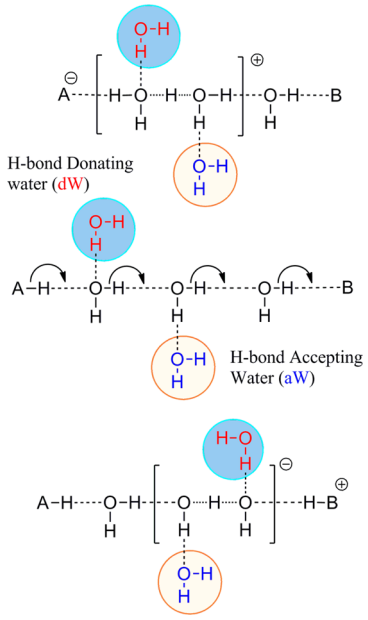

Water molecules donating (dW) and accepting (aW) H-bonds to the bridging water molecules must play an important role in the long-range proton transfer. The hydrogen-bonding structures must have different roles in the classical Grotthuss and the "proton hole" transfer mechanisms. Such hydrogen-bond donating and accepting groups may also be present in proton relay systems in enzymes, ion channels, and membrane-spanning proteins, although the long-range proton transfer in solution and biological systems can exhibit quite different molecular details depending on the pK_a values of participating groups and their interactions with the environment. Rather long "water-wires" intermittently mixed with titratable amino acid side chains, are commonly observed in the X-ray structures of biomolecules that transport protons,[32,33] and the spectroscopic signature of protonated water molecules has been captured in bacteriorhodopsin.[34] Thus, amino acid side chains certainly play an important role in the proton relay mechanism. J. M. J. Swanson et al.[16] have reviewed recent computational studies for proton transport in biomolecular systems including lipid bilayers, aquaporin water channels, and carbonic anhydrase.

The possible mechanisms of long-range proton transfer are illustrated in Scheme 2. When the end groups have extremely acidic or basic pK_a values compared with water, sequential (and

Scheme 2

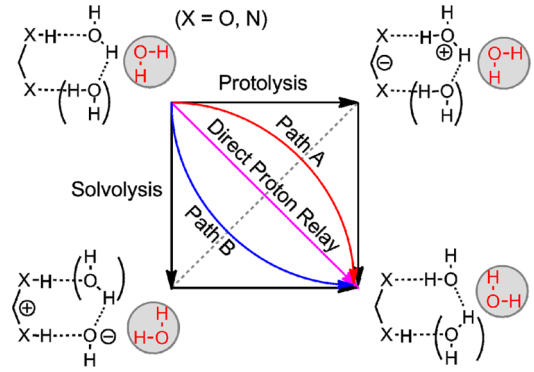

stepwise) protolysis, or solvolysis along the H-bonded wires are energetically more favorable, respectively.

However, when the end groups have moderately acidic or basic pK_a values, long-range proton transfer may occur concertedly via paths A or B through H-bonded water wires, respectively. Pathways A and B can be used as models of the intrinsic classical Grotthuss and "proton-hole" transfer mechanisms, which may operate in the proton relay systems of proteins. The "proton-hole" concept[31] was originally used for OH^- transfer in a sequential solvolysis pathway. Pathway B as a model of "proton-hole" transfer in this study does not generate an OH^- ion in its path, but forms TS that has OH^- ion character.

Although numerous experimental and theoretical studies have been performed to understand the mechanisms and dynamics of long-range proton transfer in solution, it has rarely been tried to isolate the role of solvent molecules specifically H-bonded with the water wire from overall solvent effect. Park et al.[35] have recently performed time-resolved spectroscopic studies for the excited-state double proton transfer (ESDPT) of 1:1 7-azaindole/water complex in ether, where an ether (or water) molecule is H-bonded to the mediating water. They reported that the rate constant of ESDPT becomes larger when the H-bonded ether is replaced with water, which is attributed to the enhanced proton-accepting ability of the water wire upon the H-bond formation with water. No systematic studies (experimental or theoretical) have yet been reported for the specific role of mediating water with a H-bond donating molecule to the long-range proton transfer.

Formic acid (FA) and formamidine (FN) are moderately acidic and basic compounds in aqueous solution, and cyclic monohydrated formic acid (FAW) and formamidine (FNW) complexes with additional water molecules that are H-bonded to bridging waters, as shown in Scheme 3, are one of the

Scheme 3

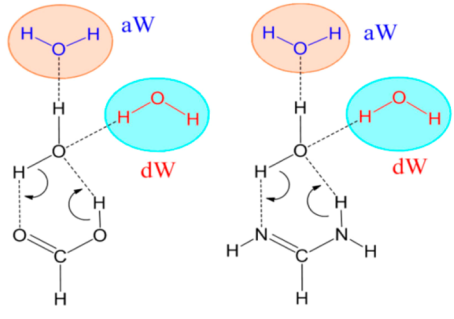

dx.doi.org/10.1021/jp310724g | J. Phys. Chem. B 2013, 117, 307−315

simplest examples of such long-range proton transfers. The mechanism and dynamics of proton transfer in FAW and FNW complexes have been extensively studied,[36−39] and these studies have shown that tunneling is very important. When the long-range proton transfer occurs in aqueous solution, bridging water molecules form hydrogen bonds with solvent molecules, as shown in Scheme 3.

The H-bond donating and accepting water molecules, denoted as dW and aW, respectively, can be used to study the different roles of H-bond solvent structures (or protein amino acid residues) on long-range proton transfer. In particular, the role of solvent structure to the TS, activation energies, and tunneling dynamics will be studied. We maintained that no water molecules were directly H-bonded to FA or FN in order to avoid any specific solvent effects. Direct dynamics with variational transition state theory including multidimensional semiclassical tunneling approximations (VTST/MT)[40] was used to determine the effects of aW and dW on the dynamics of long-range proton transfer, rate constants, and kinetic isotope effects (KIEs).

2. COMPUTATIONAL METHODS

The structures of FAW and FNW complexes were fully optimized at the B3LYP,[41] M06-2X,[42] and MP2 levels with the 6-31+G(d) and 6-311+G(d,p) basis sets using the Gaussian 09[43] package in the gas phase and in solution. Solvent effects were calculated using the integral-equation-formalism polarizable continuum model (IEFPCM)[44−46] and the Solvation Model D (SMD).[47]

Potential energy surfaces along the minimum energy path (MEP) were calculated using the direct dynamics approach with the Gaussrate[48] program, which is the interface of the Gaussian 09 and the Polyrate programs.[49] MEPs were obtained in the mass-scaled coordinate by 1 amu at the M06-2X/6-311+G(d,p) level using the Page-McIver method[50,51] and the reoriented generalized transition state theory (GTST) dividing surface algorithm.[52] Rate constants were calculated by variational transition state theory (VTST), including multidimensional tunneling. The canonical VTST rate constant is given by[53]

$$k^{\mathrm{CVT}} = \min_{s} k^{\mathrm{GT}}(T, s) = \sigma \frac{k_{\mathrm{B}}T}{h} \frac{Q^{\mathrm{GT}}(T, s_*^{\mathrm{CVT}})}{\Phi^{\mathrm{R}}} \exp[-\beta V_{\mathrm{MEP}}(s_*^{\mathrm{CVT}})] \quad (1)$$

where the superscript GT denotes the GTST; β is $1/k_{\mathrm{B}}T$; k_{B} is the Boltzmann constant; h is Planck's constant; s_*^{CVT} is the value of s at which k^{GT} is a minimum, that is, the position of the canonical variational transition state (CVT); σ is the symmetry factor; and Q^{GT} and Φ^{R} are partition functions for the generalized transition state (GTS) and reactants, respectively.

To include the tunneling effect, the calculated rate constant $k^{\mathrm{CVT}}(T)$ was multiplied by a transmission coefficient, κ

$$k^{\mathrm{CVT/G}}(T) = \kappa^{\mathrm{CVT/G}}(T) k^{\mathrm{CVT}}(T) \quad (2)$$

The transmission coefficient is defined as the ratio of the thermally averaged quantal transmission probability, $P^{\mathrm{G}}(E)$, to the thermally averaged classical transmission probability for the effective potential along the reaction coordinate that is implied by CVT theory, $P_{\mathrm{C}}^{\mathrm{CVT/G}}(E)$.[54]

$$\kappa^{\mathrm{CVT/G}}(T) = \frac{\int_0^\infty P^{\mathrm{G}}(E) e^{E/k_{\mathrm{B}}T} \mathrm{d}E}{\int_0^\infty P_{\mathrm{C}}^{\mathrm{CVT/G}}(E) e^{-E/k_{\mathrm{B}}T} \mathrm{d}E} \quad (3)$$

The value of $P_{\mathrm{C}}^{\mathrm{CVT/G}}(E)$ is unity above and zero below the classical threshold energy. Several semiclassical tunneling approximations were used to calculate $P^{\mathrm{G}}(E)$. If the reaction path was curved, tunneling was assumed to occur on the path defined by the classical turning points on the concave side of the MEP, an example of corner-cutting tunneling.[55,56] When the curvature was small, the centrifugal-dominant small-curvature semiclassical adiabatic ground state (CD-SCSAG) tunneling approximation was appropriate.[55−57] When the reaction path curvature was large, which is typical for a bimolecular light atom transfer between two heavy atoms, the large-curvature ground-state approximation, version 4 (LCG4),[58,59] was appropriate. In the LCG4 method, tunneling amplitudes were evaluated along all possible straight-line tunneling paths with equal kinetic energy before and after tunneling, and these tunneling amplitudes were weighted by the local speed and the vibrational period to give the transmission probability. The microcanonical optimized multidimensional tunneling (μOMT) approximation estimates the optimal transmission probability as the larger of the transmission probabilities evaluated by the CDSCSAG and LCG4 methods at a given energy.[60] The CD-SCSAG and LCG4 methods are called "small-curvature tunneling" (SCT) and "large-curvature tunneling" (LCT), respectively. Detailed mathematical derivations and computational formulas can be found in several reviews.[40,61,62]

3. RESULTS AND DISCUSSION

3.1. Electronic Structures. Structures of reactant and transition states (TSs) of the double proton transfer for hydrated FAW and FNW complexes in the gas phase optimized at the M06-2X/6-311+G(d,p) level are depicted in Figures 1 and 2, respectively. A water molecule makes cyclic H-bonds with FA and FN to form the monohydrated complexes, FAW and FNW, respectively. This water acts as a bridge to mediate the proton transfer between donor and acceptor. For FAW, when no aW or dW was present, the H-bond distances between FA and the bridging water, $r(O_6-H_5)$, were 1.79 and 1.15 Å at the reactant and TS, respectively. The O−H bond length of FA, $r(O_4-H_5)$, became 1.29 Å in the TS. The relatively short O_6-H_5 distance compared with O_4-H_5 indicates that an H_3O^+-like moiety with a partial positive charge was present in the TS. This would be a typical TS structure in the classical Grotthuss-type mechanism (path A in Scheme 2). In the TS of FAWaW, the O_6-H_5 and O_4-H_5 distances became even shorter and longer, respectively, than those of FAW, which suggests that aW stabilizes the H_3O^+-like moiety and increases its partial positive charge. The Mayer bond orders[63] and Löwdin partial charges[64] of the TS were calculated at the M06-2X/6-311+G(d,p) level, and some of the results are listed in Table 1. The larger bond order for O_6-H_5 compared with O_4-H_5 confirms the formation of an H_3O^+-like moiety, and the partial positive charge of the H_3O^+-like moiety became larger with the addition of H-bond accepting aW molecules. The smaller H-bond distance in the TS between aW and the bridging water, $r(O_9-H_8)$, compared with that of the reactant state, also suggest a larger partial positive charge for the H_3O^+-like moiety.

In the TS of FAWdW, however, the O_6-H_5 and O_4-H_5 distances became longer and shorter, respectively, than those of

dx.doi.org/10.1021/jp310724g | J. Phys. Chem. B 2013, 117, 307−315

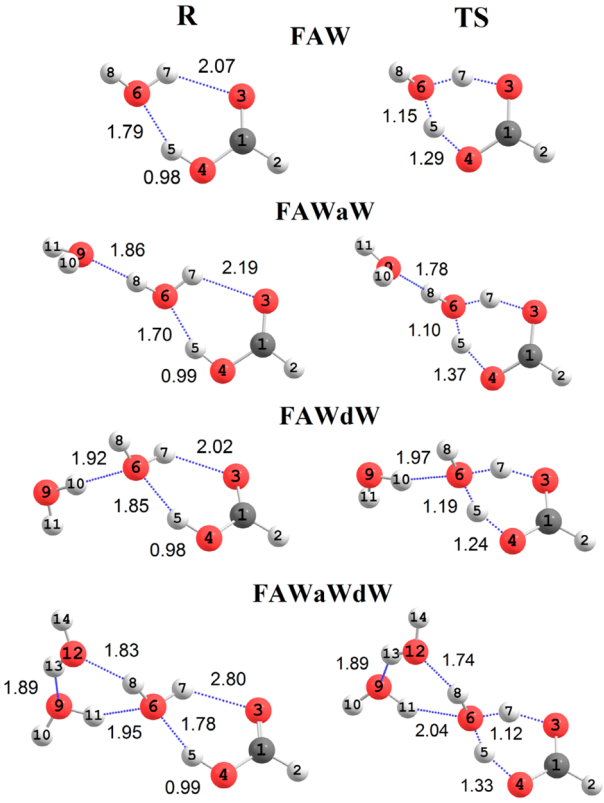

Figure 1. Structure of the reactants and TSs of hydrated FAW complexes at the M06-2X/6-311+G(d,p) level. Bond distances are in Å. Gray and red atoms represent carbon and oxygen, respectively. All TSs belong to the pathway A.

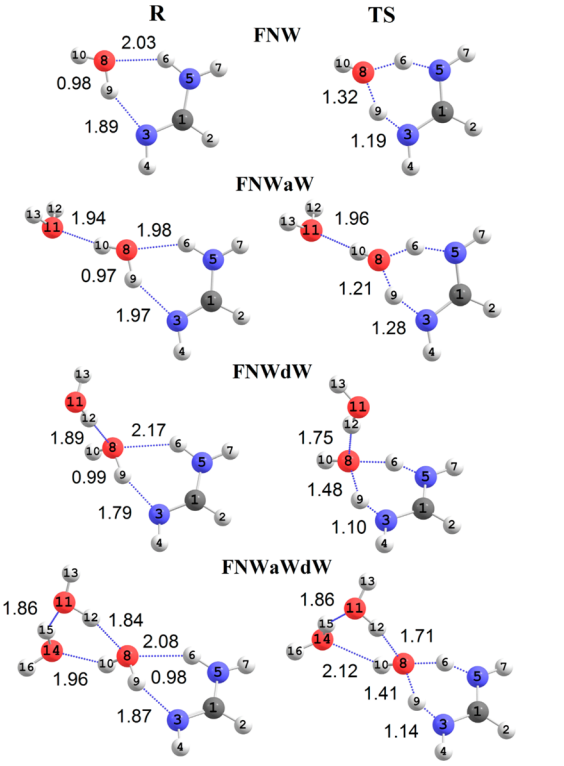

Figure 2. Structure of reactants and TSs of hydrated FNW complexes at the M06-2X/6-311+G(d,p) level. Bond distances are in Å. Blue and red atoms represent nitrogen and oxygen, respectively. The TS of FNWaW belongs to pathway A, while all others belong to pathway B.

FAW. Unlike the aW in FAW, the dW destabilized and reduced the H_3O^+ character of the TS, which resulted in a smaller partial positive charge (Table 1). The H-bond of the dW to the bridging water in the TS, $r(O_6{-}H_{10})$, became longer as the reaction proceeded from the reactant state to the TS. In FAWaWdW, both the aW and dW can form H-bonds with the bridging water to generate a cyclic water trimer. The H-bonds of the aW and dW in the TS became shorter and longer, respectively, than those of the reactant state. The $r(O_6{-}H_5)$ value in the TS of FAWaWdW was between those of FAWaW and FAWdW, as was the $r(O_4{-}H_5)$ value, because the aW and dW stabilize and destabilize the H_3O^+-like moiety of the TS, respectively, such that their contributions would mostly cancel each other. The H_3O^+ character of the TS was slightly larger than that of FAW itself, which suggests that the aW provides a slightly larger contribution to the TS structure than the dW.

In the TS of FNW, the $r(O_8{-}H_9)$ and $r(N_3{-}H_9)$ values were 1.32 and 1.19 Å, respectively, which indicates that an OH^--like moiety formed in the TS. The Mayer bond order of $O_8{-}H_9$ was smaller than that of $N_3{-}H_9$, which confirms the formation of a OH^--like moiety (Table 1). Because a proton is transferred more from water to the base to generate an anionic solvent, this type of proton transfer can be regarded as the "proton hole"-like mechanism (path B in Scheme 2). In the TS of FNWaW, the $O_8{-}H_9$ and $N_3{-}H_9$ distances became shorter and longer, respectively, than those of FNW. The former became even shorter than the latter, which suggests that the aW destabilized and reduced the OH^- character of the TS (reduced its partial negative charge). In the TS of FNWdW, however, the $O_8{-}H_9$ and $N_3{-}H_9$ distances became longer and shorter, respectively,

Table 1. Löwdin Partial Charges of H_3O^+ and OH^- Moieties as Part of the TS for Hydrated FAW and FNW Complexes, Respectively, and Mayer Bond Orders, Calculated at the M06-2X/6-311+G(d,p) Level

	$n(O_6{-}H_5)^a$	$n(O_4{-}H_5)^a$	$q(H_3O^+)^b$
FAW	0.56	0.40	0.51
FAWaW	0.66	0.31	0.62
FAWdW	0.50	0.41	0.42
	$n(O_8{-}H_9)^a$	$n(N_3{-}H_9)^a$	$q(OH^-)^b$
FNW	0.36	0.53	−0.52
FNWaW	0.50	0.41	−0.32
FNWdW	0.23	0.65	−0.72

[a]Mayer bond order. [b]Löwdin partial charge.

than those of FNW. Unlike the aW in FNW, the dW stabilized and increased the OH^- character in the TS, which is consistent with the change in the partial charges of the OH^--like moiety, as listed in Table 1.

H-bonds of the aW and dW to the bridging water, $r(O_{11}{-}H_{10})$ and $r(O_8{-}H_{12})$, in the FNWaW and FNWdW complexes, were 1.94 and 1.89 Å in the reactant state and 1.96 and 1.75 Å in the TS, respectively. The H-bond length of the dW was greatly reduced, while that of the aW changed very little, which suggests that the stabilizing effect of the dW was larger than the destabilizing effect of the aW.

3.2. Energetics of Proton Transfer. The barrier heights of FAWaW and FAWdW were smaller and larger, respectively, than that of FAW at all levels of theory used in this study (see Table 2), which indicates that the aW and dW stabilize and destabilize the TS, respectively. It is interesting that, in path A,

dx.doi.org/10.1021/jp310724g | J. Phys. Chem. B 2013, 117, 307−315

Table 2. Barrier Heights for the Double Proton Transfer at Various Levels of Theory[a]

	FAW	FAWaW	FAWdW	FAWaWdW
MP2/6-31+G(d)	17.2 (14.5)	14.3 (12.2)	18.2 (14.6)	15.8 (12.5)
MP2/6-311+G(d,p)	16.0 (13.2)	14.2 (11.9)	16.2 (12.9)	14.8 (11.7)
B3LYP/6-31+G(d)	15.0 (12.0)	12.8 (10.5)	15.7 (12.2)	14.2 (10.8)
B3LYP/6-311+G(d,p)	14.8 (11.8)	13.0 (10.5)	15.2 (11.8)	14.0 (10.8)
M06-2X/6-31+G(d)	14.9 (11.9)	12.8 (10.6)	15.6 (11.7)	14.0 (10.7)
M06-2X/6-311+G(d,p)	14.3 (11.3)	12.6 (10.1)	14.7 (11.4)	13.5 (10.2)
SMD/M06-2X/6-31+G(d,p)	11.2 (9.90)	8.56 (7.30)	12.1 (10.5)	8.76 (7.28)
SMD/M06-2X/6-311+G(d,p)	12.4 (11.2)	9.63 (8.59)	13.5 (11.9)	9.71 (8.74)
IEFPCM/M06-2X/6-31+G(d,p)	11.8 (9.51)	9.63 (7.91)	12.8 (9.73)	10.4 (8.07)
IEFPCM/M06-2X/6-311+G(d,p)	13.4 (11.1)	11.2 (9.16)	14.4 (11.0)	12.0 (9.52)
	FNW	FNWaW	FNWdW	FNWaWdW
MP2/6-31+G(d)	19.7 (16.6)	22.2 (17.8)	13.9 (12.4)	16.8 (14.3)
MP2/6-311+G(d,p)	20.0 (15.8)	20.8 (16.3)	15.6 (13.3)	17.6 (14.1)
B3LYP/6-31+G(d)	17.3 (14.1)	19.9 (15.4)	12.4 (10.9)	14.7 (12.3)
B3LYP/6-311+G(d,p)	17.3 (13.9)	19.3 (14.7)	12.9 (11.3)	14.9 (12.4)
M06-2X/6-31+G(d)	18.3 (14.8)	19.5 (15.2)	14.0 (11.4)	16.5 (13.6)
M06-2X/6-311+G(d,p)	17.9 (14.1)	18.6 (14.6)	14.2 (11.2)	16.4 (13.1)
SMD/M06-2X/6-31+G(d,p)	11.2 (11.0)	12.6 (12.4)	7.38 (6.70)	8.49 (8.17)
SMD/M06-2X/6-311+G(d,p)	11.5 (11.5)	13.1 (13.1)	7.55 (7.15)	9.26 (8.66)
IEFPCM/M06-2X/6-31+G(d,p)	13.7 (11.9)	15.9 (13.4)	9.01 (7.85)	9.30 (7.89)
IEFPCM/M06-2X/6-311+G(d,p)	14.5 (13.0)	16.9 (14.7)	9.81 (8.93)	10.2 (9.05)

[a]The numbers in parentheses include zero-point energies.

the stabilizing effect in activation energy was always larger than the destabilizing effect in absolute amount. In contrast, the barrier heights of FNWaW and FNWdW were larger and smaller, respectively, than that of FNW, which indicates that the aW and dW destabilize and stabilize the TS, respectively. In this case, the stabilizing effect of the dW was larger than the destabilizing effect of the aW in the energy barrier of path B.

In the FAWaWdW and FNWaWdW complexes, the barrier heights were slightly larger than the most stable ones for the FAWaW and FNWdW complexes, respectively. These results suggest that in long-range proton transfer, the bridging water needs only a single H-bond donating or accepting solvent molecule (or functional group in a protein), depending on the mechanism (path A or path B) of the most efficient process, and any additional H-bond donating or accepting molecules (or groups) would not further aid proton transfer. Dielectric continuum calculations were carried out to include solvent effects (water) using the IEFPCM and SMD methods. All activation energies in solution were smaller than the corresponding values in the gas phase. The effects of H-bond accepting and donating water molecules in the water environment were in general consistent with the effects observed in the gas phase: aW and dW reduced and increased the barrier heights of Grotthuss-type proton transfer (path A), respectively, and increased and reduced those of "proton hole"-like transfer (path B), respectively.

3.3. Dynamics of Double Proton Transfer. Figure 3 shows the vibrationally adiabatic ground-state energies along

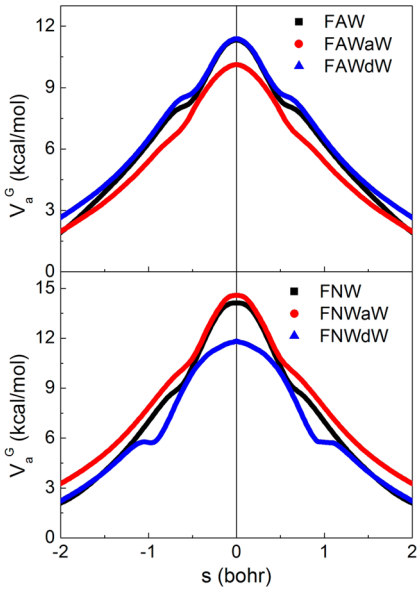

Figure 3. Adiabatic ground-state energy curves along the MEP for double proton transfer processes of hydrated FAW and FNW complexes.

the MEP for long-range proton transfer processes in the hydrated FAW and FNW complexes (all Born–Oppenheimer potential and adiabatic energy curves of hydrated FAW and FNW systems are shown in Figures S1 and S2, respectively). The vibrationally adiabatic energy, V_a^G, is the sum of the Born–Oppenheimer potential, V_{MEP}, and the local zero-point energies. No stable intermediates were observed in the potential and adiabatic energy curves along the reaction coordinate, which indicates that the two protons were transferred concertedly. In path A, the adiabatic energy curves of FAW and FAWdW were nearly overlapped around the top of the barrier. The FAWaW curve was below the other two curves, and its width near the TS was wider than the other two curves. The imaginary frequencies for the reaction coordinate motion at the TS of FAW, FAWaW, and FAWdW complexes were 1364, 869, and 1607 cm^{-1}, respectively, which means that the potential energy barriers of FAWaW and FAWdW were the widest and narrowest, respectively. In path B, the FNWdW curve was lower and wider than the curves of FNW and FNWaW. The imaginary frequencies of FNW, FNWaW, and FNWdW were 1380, 1645, and 455 cm^{-1}, respectively. The wider adiabatic energy curves near the transition state were generally expected to give lower tunneling probabilities.

dx.doi.org/10.1021/jp310724g | J. Phys. Chem. B 2013, 117, 307–315

The changes in bond lengths involving the proton in motion along the MEP of path A for hydrated FAW complexes are shown in Figure 4. As the reaction proceeded from reactant ($s = -\infty$) to product ($s = +\infty$), the H_5 atom of formic acid rarely moved until it reached approximately s = −0.75, where it started moving very rapidly from O_4 in the six-membered H-bonded ring to O_6, and the $r(O_4–H_5)$ and $r(O_6–H_5)$ values crossed at approximately $s = -0.2$ bohr, whereas the H_7 atom of the mediating water moved rather slowly from O_6 to O_3, and the $r(O_6–H_7)$ and $r(O_3–H_7)$ values crossed at approximately $s = 0.2$ bohr (path A). The two protons moved very rapidly and asynchronously in the region $-0.75 < s < 0.75$. These crossing points of $r(O_4–H_5)$ and $r(O_6–H_5)$ in the MEP for the FAWaW and FAWdW complexes occurred around $s = -0.35$ and −0.07 bohr, respectively. The larger the absolute s value of the crossing point, the longer the H_3O^+-moiety existed in the intrinsic reaction path, which means that the H-bond accepting water (aW) not only lowered the activation barrier, but it increased the asynchronicity of the long-range proton transfer. However, in the FAWdW complex, the crossing point came very close to the conventional TS ($s = 0$), which suggests that the H-bond donating water (dW) executed a nearly synchronous proton transfer and increased the activation energy as well.

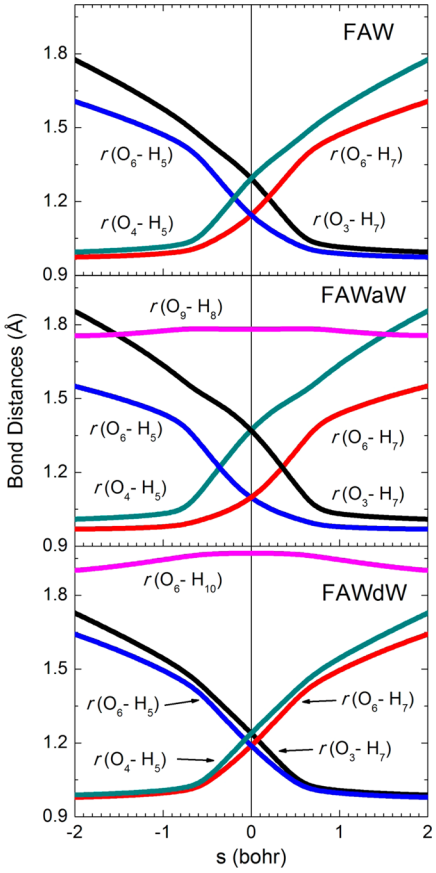

Figure 4. Several bond distances in Å along the reaction coordinate of the double proton transfer in hydrated FAW complexes.

In the FNW complexes, the change in bond distances was also divided into two parts: from the reactant ($s = -\infty$) to around $s = -0.7$ bohr and from the product ($s = +\infty$) to around $s = 0.7$ bohr, no notable changes in N–H and O–H bond distances were observed, and in the region $-0.75 < s < 0.75$, rapid proton transfer occurred. The H_9 atom of the mediating water started moving first in this case (path B), and the crossing points of $r(O_8–H_9)$ and $r(N_3–H_9)$ values were around $s = -0.18$ bohr. These crossing points in the FNWaW and FNWdW complexes were around $s = 0.1$ and −0.55, respectively. The aW and dW, contrary to their role in the FAW complexes, reduced and increased the asynchronicity of the double proton transfer in the FNW complexes, respectively. For both FAW and FNW complexes, the lower the activation energy of the double proton transfer, the larger the asynchronicity became. As clearly seen in Figures 4 and 5, synchronicity of the double proton transfer was highly dependent on the dW and aW bound to the bridging water of the FAW and FNW complexes.

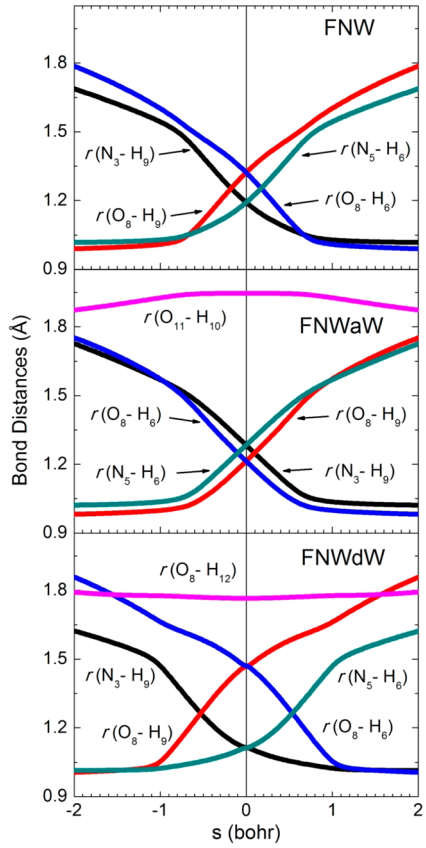

Figure 5. Several bond distances in Å along the reaction coordinate of the double proton transfer in hydrated FNW complexes.

The change in the H-bond distances of aW and dW to the bridging water were plotted along the MEP, which is also shown in Figures 4 and 5 for the hydrated FAW and FNW complexes, respectively. Interestingly, the $O_9–H_8$ and $O_8–H_{12}$ H-bonds stabilizing the activation energies of the FAWaW and FNWdW complexes, respectively, rarely changed near the transition state, while the $O_6–H_{10}$ and $O_{11}–H_{10}$ H-bonds destabilizing those activation energies significantly changed near the transition state. These H-bonded water molecules (aW and dW) play an important role in the tunneling dynamics as described later.

3.4. Rate Constants and Kinetic Isotope Effects. The rate constants with and without tunneling calculated by VTST/MT at 298 K for HH transfers are listed in Table 3. The dependence of variational effect on temperature was very small

dx.doi.org/10.1021/jp310724g | J. Phys. Chem. B 2013, 117, 307–315

Table 3. Rate Constants (s^{-1}), Tunneling Coefficients, and Arrhenius Activation Energies (kcal/mol) for the Double Proton Transfer Calculated by Direct Ab Initio Reaction Dynamics with VTST/MT at the M06-2X/6-311+G(d,p) Level at 298 K

	k_{HH}^{CVT}	$\kappa_{HH}^{\mu OMT}$	$k_{HH}^{CVT/\mu OMT}$	E_a
FAW	5.44×10^3	9.57	5.20×10^4	8.02
FAWaW	3.18×10^4	5.79	1.84×10^5	7.47
FAWdW	1.45×10^3	6.33	9.20×10^3	8.43
FAWaWdW	2.93×10^4	6.99	2.05×10^5	7.62
FNW	3.89×10^1	21.1	8.22×10^2	9.29
FNWaW	1.14×10^1	13.0	1.48×10^2	10.4
FNWdW	3.37×10^3	5.58	1.88×10^4	8.74
FNWaWdW	1.88×10^2	11.8	2.22×10^3	8.99

in these reactions, such that only the CVT rate constants are listed. The Arrhenius activation energies were also calculated from the rate constants between 250 and 400 K. The transmission coefficients using the SCT, LCT, and μOMT approximations were calculated and the SCT tunneling coefficients were always larger than the LCT values and determined μOMT coefficients. This means that the reaction path curvatures were not very large, although these systems have the heavy−light−heavy mass combination. Transmission coefficients using the μOMT approximation are listed in Table 3. All tunneling coefficients, rate constants for HH and DD transfers, and HH/DD KIEs are listed in Tables S1−S3 in the Supporting Information.

The tunneling coefficients ($\kappa^{\mu OMT}$) for the double proton transfer in both the FAW and FNW complexes were quite large. The tunneling coefficient for the FAW, FAWaW, FAWdW complexes was 9.57, 5.79, and 6.33, respectively. It is interesting that in all cases water molecules H-bonded to the bridging water reduced the tunneling effect. The barrier height of FAWaW was lower than that of FAW, thus the barrier became wider (Figure 3), which reduced the tunneling coefficient. The barrier of FAWdW had nearly the same activation energy as that of FAW (Table 2), but it had a larger imaginary frequency with a highly synchronous proton transfer. One might expect that the tunneling coefficient would be larger in this case and increase the rate constant to some extent; however, the $\kappa^{\mu OMT}$ value of FAWdW was smaller than that of FAW. This result may originate from the effective mass of transferring protons being increased by the dW molecule. As shown in Figure 4, the H-bond distance of the dW to the bridging water changed significantly near the transition state, which means that the dW motion was coupled with the hydrogenic motion of the double proton transfer through H-bonds. This coupling would increase the effective mass of the transferring hydrogen atoms, resulting in a smaller tunneling effect.

The tunneling coefficients for the FNW, FNWaW, and FNWdW complexes were 21.1 13.0, and 5.58, respectively. Again, in the FNWdW complex, the tunneling effect was reduced due to the lower and wider barrier. However, in the FNWaW complex, the $\kappa^{\mu OMT}$ value became smaller even though the barrier was higher and narrower. The H-bond distance of the aW to the bridging water changed significantly near the transition state as shown in Figure 5. Therefore, the aW motion was coupled with the hydrogenic motion of the double proton transfer in this case, and increased the effective mass of the transferring hydrogen atoms to reduce the tunneling effect. When a barrier becomes higher, in general its width becomes narrower giving a larger tunneling effect, which increases the rate constant. Therefore, tunneling can compensate to some extent for a reduced rate constant due to an increased activation energy. However, such effects were not observed in the long-range proton transfer with a solvent molecule H-bonded to the water-wire. All water molecules interacting with the mediating water, whether they raised or reduced the barrier, appeared to reduce tunneling.

In the ESDPT of 1:1 7-azaindole/water complex in ether,[35] the rate constants were increased 230 times compared with the corresponding theoretical values in the gas phase.[65] Solvent effect lowered the activation energies of ESDPT to increase the reaction rate. The KIE in ether was 1.8 at 293 K, whereas the theoretically estimated KIE in the gas phase was 4.0 at 298 K.[65] The increased tunneling mass due to the H-bonded ether with water wire would result in smaller tunneling probabilities to give small KIE in ether. These results are consistent with smaller KIEs of FAWaW resulting from smaller tunneling coefficients due to H-bond accepting water bound to water wire. The quasiclassical KIE without tunneling, which originates from the ZPE energy change between reactant and TS, was about 2.5 in the gas phase. The KIE in ether, which is slightly smaller than the predicted quasiclassical value in the gas phase, suggests that tunneling contribution to the KIE might be negligible in ether.

Rate constants including tunneling of FAW at 298 K were on the order of 10^5 s^{-1}. In the Grotthuss mechanism of long-range proton transfer (path A), the rate constant is largest when the mediating water has only a single H-bond accepting water (FAWaW), while in the "proton hole"-like mechanism, the rate was fastest when the mediating water has a single H-bond donating water (FNWdW). Nature follows the most efficient pathway, thus, the dW in path A and the aW in path B would not be utilized for long-range proton transfer, although they must transiently be bound to the water wire in aqueous solution. These results suggest that the classical Grotthuss and the "proton hole"-like mechanisms, which may occur in the proton relay systems in proteins, require quite different solvent (or protein) environments for the most efficient processes. For complexes that form a cyclic water trimer with the mediating water (FAWaWdW and FNWaWdW), the Arrhenius activation energies at 298 K were slightly larger than those of FAWaW and FNWdW, respectively; however, the formation of a water trimer must entropically be very unfavorable. The primary KIEs at 298 K are shown in Table 4. The HH/DD KIE including tunneling was 13.4 for the FAWaW complex, which is in good agreement with experimental KIE values for acetic acid and methanol (KIE = 15 at 298 K).[66] The KIEs of hydrated FNW

Table 4. HH/DD KIEs and the Ratio of Tunneling Coefficients at 298 K

	$k_{HH}^{CVT}/k_{DD}^{CVT}$	$\kappa_{HH}^{\mu OMT}/\kappa_{DD}^{\mu OMT}$	$k_{HH}^{CVT/\mu OMT}/k_{DD}^{CVT/\mu OMT}$
FAW	8.42	2.25	18.9
FAWaW	5.78	2.33	13.4
FAWdW	10.7	1.43	15.3
FAWaWdW	7.67	2.00	15.3
FNW	10.4	4.20	43.7
FNWaW	12.3	2.98	36.5
FNWdW	5.37	2.82	15.2
FNWaWdW	7.93	3.66	29.2

dx.doi.org/10.1021/jp310724g | J. Phys. Chem. B 2013, 117, 307−315

complexes were, in general, much larger than those of hydrated FAW complexes; however, the KIE value of the most efficient "proton hole"-like pathway (KIE = 15 for FNWdW) was very similar to that of the most efficient Grotthuss pathway (KIE = 13 for FAWaW).

4. CONCLUDING REMARKS

We have studied the role of solvent molecules in the TS that are H-bonded to the mediating water in long-range proton transfers using a direct ab initio dynamics approach with variational transition-state theory including multidimensional tunneling. When the end groups have acidic or basic pK_a values, the classical Grotthuss and proton-hole transfer mechanisms were energetically most favorable, respectively. In the Grotthuss mechanism, the rate constant was the largest when the mediating water has a single H-bond accepting water (FAWaW), while in the "proton hole"-like mechanism, the rate was fastest when the mediating water has a single H-bond donating water (FNWdW). These results suggest that the classical Grotthuss and "proton hole"-like mechanisms require quite different environments in the TS for the most efficient processes, and that the bridging water needs only a single H-bond donating or accepting solvent molecule (or protein functional group), depending on the mechanism, for the most efficient process, and any additional H-bond donating or accepting molecules (or groups) might not assist the proton transfer. The synchronicity of double proton transfer was highly dependent on solvent molecules bound to the bridging water. For both FAW and FNW complexes, the lower the activation energy of the double proton transfer, the larger the asynchronicity became.

Tunneling was very important to double proton transfer and depended greatly on the water molecules associated with the water wire at the TS. All molecules bound to the bridging water reduced the tunneling probability, even as they narrowed the barrier width and increased the synchronicity of proton transfer, which was attributed to the effective mass of transferring protons increasing due to the coupled motion of the H-bonded water with the proton being transferred. The theoretical HH/DD KIE, including tunneling, was in good agreement with the experimentally derived KIE. The KIE values from the most efficient Grotthuss and "proton hole"-like pathways were not very different.

■ ASSOCIATED CONTENT

Supporting Information

Potential and adiabatic ground-state energy curves along the MEP for proton transfer processes of all hydrated FAW and FNW complexes, and rate constants and tunneling coefficients calculated by VTST/MT in the temperature range 250−450 K for double proton and deuterium transfers are provided. This material is available free of charge via the Internet at http://pubs.acs.org.

■ AUTHOR INFORMATION

Corresponding Author

*E-mail: yhkim@khu.ac.kr.

Notes

The authors declare no competing financial interest.

■ ACKNOWLEDGMENTS

We thank Professor Donald G. Truhlar for providing the Gaussrate and Polyrate programs. This work was supported by a grant from the Korea Research Foundation (KRF Grant No. 2012-0003010). We are pleased to acknowledge support in the form of computing resources from the Center for Academic Computing at Kyung Hee University.

■ REFERENCES

(1) Bender, M. L. *Mechanisms of Homogeneous Catalysis from Protons to Proteins*; John Wiley and Sons: New York, 1971.
(2) Melander, L.; Saunders, W. H. *Reaction Rates of Isotopic Molecules*; John Wiley and Sons: New York, 1980.
(3) Tuckerman, M. E.; Marx, D.; Parrinello, M. *Nature* **2002**, *417* (6892), 925−929.
(4) Gutman, M.; Nachliel, E. *Annu. Rev. Phys. Chem.* **1997**, *48*, 329−356.
(5) Mathias, G.; Marx, D. *Proc. Natl. Acad. Sci. U.S.A.* **2007**, *104* (17), 6980−6985.
(6) Royant, A.; Edman, K.; Ursby, T.; Pebay-Peyroula, E.; Landau, E. M.; Neutze, R. *Nature* **2000**, *406* (6796), 645−648.
(7) Faxen, K.; Gilderson, G.; Adelroth, P.; Brzezinski, P. *Nature* **2005**, *437* (7056), 286−289.
(8) Agmon, N. *Chem. Phys. Lett.* **1995**, *244* (5−6), 456−462.
(9) Luecke, H.; Richter, H.-T.; Lanyi, J. K. *Science* **1998**, *280* (5371), 1934−1937.
(10) Kuhlbrandt, W. *Nature* **2000**, *406* (6796), 569−570.
(11) Decoursey, T. E. *Physiol. Rev.* **2003**, *83* (2), 475−579.
(12) Lu, D.; Voth, G. A. *J. Am. Chem. Soc.* **1998**, *120* (16), 4006−4014.
(13) Vuilleumier, R.; Borgis, D. *J. Phys. Chem. B* **1998**, *102* (22), 4261−4264.
(14) Mei, H. S.; Tuckerman, M. E.; Sagnella, D. E.; Klein, M. L. *J. Phys. Chem. B* **1998**, *102* (50), 10446−10458.
(15) Pomès, R.; Roux, B. *Biophys. J.* **2002**, *82* (5), 2304−2316.
(16) Swanson, J. M. J.; Maupin, C. M.; Chen, H.; Petersen, M. K.; Xu, J.; Wu, Y.; Voth, G. A. *J. Phys. Chem. B* **2007**, *111* (17), 4300−4314.
(17) Borgis, D.; Hynes, J. T. *Chem. Phys.* **1993**, *170* (3), 315−346.
(18) Marx, D.; Tuckerman, M. E.; Hutter, J.; Parrinello, M. *Nature* **1999**, *397* (6720), 601−604.
(19) Geissler, P. L.; Dellago, C.; Chandler, D.; Hutter, J.; Parrinello, M. *Science* **2001**, *291* (5511), 2121−2124.
(20) Cukier, R. I.; Nocera, D. G. *Annu. Rev. Phys. Chem.* **1998**, *49*, 337−369.
(21) Agarwal, P. K.; Webb, S. P.; Hammes-Schiffer, S. *J. Am. Chem. Soc.* **2000**, *122* (19), 4803−4812.
(22) Cui, Q.; Karplus, M. *J. Phys. Chem. B* **2002**, *106* (32), 7927−7947.
(23) Cox, M. J.; Timmer, R. L. A.; Bakker, H. J.; Park, S.; Agmon, N. *J. Phys. Chem. A* **2009**, *113* (24), 6599−6606.
(24) Cox, M. J.; Bakker, H. J. *J. Chem. Phys.* **2008**, *128* (17), 174501−10.
(25) Weller, A. *Prog. React. Kinet.* **1961**, *1*, 188−213.
(26) Mohammed, O. F.; Pines, D.; Nibbering, E. T. J.; Pines, E. *Angew. Chem., Int. Ed.* **2007**, *119* (9), 1480−1483.
(27) Mohammed, O. F.; Pines, D.; Dreyer, J.; Pines, E.; Nibbering, E. T. J. *Science* **2005**, *310* (5745), 83−86.
(28) de Grotthuss, C. J. T. *Ann. Chim. Phys.* **1806**, *58*, 54−73.
(29) Eigen, M. *Angew. Chem., Int. Ed. Engl.* **1964**, *3* (1), 1−19.
(30) Riccardi, D.; Konig, P.; Prat-Resina, X.; Yu, H.; Elstner, M.; Frauenheim, T.; Cui, Q. *J. Am. Chem. Soc.* **2006**, *128* (50), 16302−16311.
(31) Tuckerman, M. E.; Chandra, A.; Marx, D. *Acc. Chem. Res.* **2006**, *39* (2), 151−158.
(32) Schultz, B. E.; Chan, S. I. *Annu. Rev. Biophys. Biomol. Struct.* **2001**, *30*, 23−65.

(33) Luecke, H.; Lanyi, J. K. In *Advances in Protein Chemistry*, Douglas, C. R., Ed.; Academic Press: New York, 2003; Vol. *63*, pp 111−130.
(34) Garczarek, F.; Gerwert, K. *Nature* **2006**, *439* (7072), 109−112.
(35) Park, S.-Y.; Jeong, H.; Jang, D.-J. *J. Phys. Chem. B* **2011**, *115* (19), 6023−6031.
(36) Bell, R. L.; Truong, T. N. *J. Phys. Chem. A* **1997**, *101* (42), 7802−7808.
(37) Kim, Y. *J. Am. Chem. Soc.* **1996**, *118* (6), 1522−1528.
(38) Kim, Y. *J. Phys. Chem. A* **1998**, *102* (18), 3025−3036.
(39) Kim, Y.; Lim, S.; Kim, H.-J.; Kim, Y. *J. Phys. Chem. A* **1999**, *103* (5), 617−624.
(40) Truhlar, D. G.; Isaacson, A. D.; Garrett, B. C. In *Theory of Chemical Reaction Dynamics*; Baer, M., Ed.; CRC Press: Boca Raton, FL, 1985; Vol. *4*, pp 65−137.
(41) Becke, A. D. *J. Chem. Phys.* **1993**, *98* (7), 5648−5652.
(42) Zhao, Y.; Truhlar, D. *Theor. Chem. Acc.* **2008**, *120* (1), 215−241.
(43) Frisch, M. J., et al. *Gaussian 09*; Gaussian, Inc.: Wallingford, CT, 2009.
(44) Cossi, M.; Barone, V.; Mennucci, B.; Tomasi, J. *Chem. Phys. Lett.* **1998**, *286* (3−4), 253−260.
(45) Mennucci, B.; Tomasi, J. *J. Chem. Phys.* **1997**, *106* (12), 5151−5158.
(46) Cances, E.; Mennucci, B.; Tomasi, J. *J. Chem. Phys.* **1997**, *107* (8), 3032−3041.
(47) Marenich, A. V.; Cramer, C. J.; Truhlar, D. G. *J. Phys. Chem. B* **2009**, *113* (18), 6378−6396.
(48) Zheng, J.; Zhang, S.; Corchado, J. C.; Chuang, Y.-Y.; Coitiño, E. L.; Ellingson, B. A.; Truhlar, D. G. *Gaussrate 2009-A*; University of Minnesota: Minneapolis, MN, 2010.
(49) Zheng, J., et al. *Polyrate 2010-A*; University of Minnesota: Minneapolis, MN, 2010.
(50) Page, M.; McIver, J. J. W. *J. Chem. Phys.* **1988**, *88* (2), 922−935.
(51) Page, M.; Doubleday, C.; McIver, J. J. W. *J. Chem. Phys.* **1990**, *93* (8), 5634−5642.
(52) Villa, J.; Truhlar, D. G. *Theor. Chem. Acc.* **1997**, *97* (1), 317−323.
(53) Garrett, B. C.; Joseph, T.; Truong, T. N.; Truhlar, D. G. *Chem. Phys.* **1989**, *136* (2), 271−293.
(54) Garrett, B. C.; Truhlar, D. G.; Grev, R. S.; Magnuson, A. W. *J. Phys. Chem.* **1980**, *84* (13), 1730−1748.
(55) Liu, Y. P.; Lynch, G. C.; Truong, T. N.; Lu, D. H.; Truhlar, D. G.; Garrett, B. C. *J. Am. Chem. Soc.* **1993**, *115* (6), 2408−2415.
(56) Skodje, R. T.; Truhlar, D. G.; Garrett, B. C. *J. Phys. Chem.* **1981**, *85* (21), 3019−3023.
(57) Lu, D.-h.; Truong, T. N.; Melissas, V. S.; Lynch, G. C.; Liu, Y.-P.; Garrett, B. C.; Steckler, R.; Isaacson, A. D.; Rai, S. N.; Hancock, G. C.; Lauderdale, J. G.; Joseph, T.; Truhlar, D. G. *Comput. Phys. Commun.* **1992**, *71* (3), 235−262.
(58) Fernandez-Ramos, A.; Truhlar, D. G. *J. Chem. Phys.* **2001**, *114* (4), 1491−1496.
(59) Fernández-Ramos, A.; Truhlar, D. G.; Corchado, J. C.; Espinosa-García, J. *J. Phys. Chem. A* **2002**, *106* (19), 4957−4960.
(60) Liu, Y. P.; Lu, D. H.; Gonzalez-Lafont, A.; Truhlar, D. G.; Garrett, B. C. *J. Am. Chem. Soc.* **1993**, *115* (17), 7806−7817.
(61) Garrett, B. C.; Truhlar, D. G. In *Theory and Applications of Computational Chemistry: The First Forty Years*; Dykstra, C. E., Frenking, G., Kim, K. S., Scuseria, G. E., Eds.; Elsevier: Amsterdam, 2005; pp 67−87.
(62) Fernandez-Ramos, A.; Ellingson, B. A.; Garrett, B. C.; Truhlar, D. G. In *Reviews in Computational Chemistry*; Lipkowitz, K. B., Cundari, T. R., Eds.; Wiley-VCH: Hoboken, NJ, 2007; Vol. *23*, pp 125−232.
(63) Mayer, I. *Chem. Phys. Lett.* **1983**, *97* (3), 270−274.
(64) Lowdin, P.-O. *J. Chem. Phys.* **1950**, *18* (3), 365−375.
(65) Duong, M. P. T.; Kim, Y. *J. Phys. Chem. A* **2010**, *114* (10), 3403−3410.
(66) Gerritzen, D.; Limbach, H. H. *J. Am. Chem. Soc.* **1984**, *106* (4), 869−879.